ORIGINAL RESEARCH

Characterization of Aluminum Oxide–Hydroxyapatite Ceramic Composites Sintered with Hydroxyapatite at Various Concentrations and Post-sinter Degradation By-products Analysis: An *In Vitro* Spectroscopic Study

Kandasamy Balu[1], Jailaudeen Yasmin-Fathima[2], Ranganathan Ajay[3]

Received on: 02 October 2024; *Accepted on:* 12 November 2024; *Published on:* 13 March 2025

Abstract

Aim: To characterize newly formulated aluminum oxide–hydroxyapatite (AHA) ceramic composites sintered with hydroxyapatite (HA) incorporated at four different concentrations and to ascertain the absence of post-sinter degradation by-products in the ceramic composite.

Materials and methods: Control group A contains plain sintered aluminum oxide (Al_2O_3). Four experimental groups were formulated and sintered by admixing HA with Al_2O_3 at 2.5 wt% (group B), 5.0 wt% (group C), 7.5 wt% (group D), and 10 wt% (group E) concentrations. Field emission scanning electron microscopy (FESEM) combined with energy dispersive X-ray (EDX) spectroscopy were employed for surface topographical and elemental composition analysis, respectively. To detect post-sinter degradation by-products, X-ray diffraction (XRD) spectroscopy of ground specimens was performed.

Results: Hydroxyapatite hexagonal crystallites were absent in the control group and were observed in all the experimental groups. There were significant differences in the EDX spectra between the control and the experimental groups. EDX spectra showed peaks of calcium (Ca), phosphorus (P), and calcium aluminates (CA) in all the experimental groups, thereby ascertaining the presence of undecomposed HA. An exclusive peak corresponding to krotite appeared only in groups D and E.

Conclusion: The newly formulated AHA ceramic composites sintered with incorporated HA in all four concentrations do not contain post-sinter degradation by-products, and the HA was not decomposed when sintered with Al_2O_3.

Clinical significance: Neither with any prior surface treatment nor with the use of primers, this novel attempt would be beneficial in chemically bonding alumina-based ceramics with 10-methacryloxydecyl dihydrogen phosphate (10-MDP)-containing resin cements, thereby increasing the clinical serviceability of the prostheses.

Keywords: Aluminum oxide, Calcium aluminate, Ceramic composite, Chemical characterization, Hydroxyapatite.

World Journal of Dentistry (2025): 10.5005/jp-journals-10015-2501

Introduction

The growing interest in esthetic dentistry has focused numerous studies on dental ceramics due to their unique mechanical, chemical, esthetic, and biological properties.[1] Depending on the chemical composition, ceramics can be classified as oxide ceramics [aluminum oxide (Al_2O_3), zirconium oxide (ZrO_2)-based] and glass ceramics [silica (SiO_2)-based]. The stable chemical structure of oxide ceramics has led to significant improvements in their mechanical properties, referred to as high-strength core ceramics.[2] Although superior in terms of performance, the bonding of oxide ceramics to luting agents remains a challenge due to their nonpolar properties.[3] Al_2O_3 ceramics need surface alterations to chemically bond with 10-methacryloxydecyl dihydrogen phosphate (10-MDP)-based cement. Moreover, previous studies cannot provide direct evidence of the chemical bonding between 10-MDP and ZrO_2 ceramics.[4] Numerous methods that aim to alter the surface characteristics have been explored to increase the bondability of oxide ceramics, including air abrasion, acid etching, SiO_2 coating, laser irradiation, etc.[5] Because of the absence of a silicon oxide phase, acid etching and silanization are unreliable treatments for oxide ceramics.[6] Furthermore, there is controversy regarding the effects of air abrasion on bonding because it may lead to crack development.[7] Although the above approaches have been partly successful, there is no unanimity on the best surface treatment yet.[8]

Hydroxyapatite (HA) has gained greater significance as a biomaterial in prosthetic and restorative dentistry due to its biocompatibility, radiopacity, abrasion resistance, hardness, interfacial surface tension, and wettability.[9] The antibacterial

[1–3]Department of Prosthodontics and Crown and Bridge, Vivekanandha Dental College for Women, Namakkal, Tamil Nadu, India

Corresponding Author: Ranganathan Ajay, Department of Prosthodontics and Crown and Bridge, Vivekanandha Dental College for Women, Namakkal, Tamil Nadu, India, Phone: +91 8754120490, e-mail: jrangclassiq@gmail.com

How to cite this article: Balu K, Yasmin-Fathima J, Ajay R. Characterization of Aluminum Oxide–Hydroxyapatite Ceramic Composites Sintered with Hydroxyapatite at Various Concentrations and Post-sinter Degradation By-products Analysis: An *In Vitro* Spectroscopic Study. World J Dent 2025;16(1):8–13.

Source of support: Nil

Conflict of interest: None

© The Author(s). 2025 Open Access. This article is distributed under the terms of the Creative Commons Attribution 4.0 International License (https://creativecommons.org/licenses/by-nc/4.0/), which permits unrestricted use, distribution, and non-commercial reproduction in any medium, provided you give appropriate credit to the original author(s) and the source, provide a link to the Creative Commons license, and indicate if changes were made. The Creative Commons Public Domain Dedication waiver (http://creativecommons.org/publicdomain/zero/1.0/) applies to the data made available in this article, unless otherwise stated.

effect[10] and tensile strength[11] of HA added to dental ceramics are well documented in previous studies. The chemical bonding between 10-MDP and HA has been explained by Fukegawa et al.[12] For many years, numerous techniques have been introduced for the deposition of HA to modify the surface of prosthetic materials such as dental implants and dental ceramics, including thermal coating, plasma spraying, sol–gel deposition, aerosol deposition, etc. However, it is important to note that each method could change the mechanical properties of the parent material, and the coating was susceptible to contamination, delamination, and disintegration, which would greatly influence the bond strength.[13] Hence, it would be a breakthrough to blend the dental ceramics and HA into a composite ceramic material with a chemical bonding ability facilitated by 10-MDP at the adhesive resin-ceramic interface.

Previous attempts have been made to improve the properties of ZrO_2 by incorporating HA.[14,15] Despite the superior mechanical properties, HA decomposition was observed during high-temperature sintering of ZrO_2, resulting in the formation of decomposed by-products such as alpha-tricalcium phosphate (α-TCP), beta-tricalcium phosphate (β-TCP), calcium oxide (CaO), and tetracalcium phosphate (TTCP). Such decomposition inadvertently affected the properties of ZrO_2 through poor densification and degradation.[16] The incorporation of HA in Al_2O_3 and characterization of the resultant Al_2O_3–HA (AHA) composite ceramic has hardly been reported in the dental literature. Due to the lower sintering temperature of Al_2O_3 compared to ZrO_2, the incorporation of HA in the former shall be experimented with. At low sintering temperatures, the presence of post-sinter degradable by-products was presumed to be negligible. Such incorporation would be hypothetically beneficial in promoting chemical adhesion between dental aluminous ceramic prostheses and 10-MDP-containing self-adhesive resin cement. Hence, the present research aims to chemically characterize the surface topography of the novel AHA ceramic composite and to confirm the absence of post-sinter decomposition by-products.

Materials and Methods

The present *in vitro* study was conducted at Vivekanandha Dental College for Women, Tiruchengode, for 6 months (November 2023–May 2024) after obtaining institutional approval. The research comprised five groups: a control group (group A) with Al_2O_3 without HA, and four experimental groups (groups B, C, D, and E) with Al_2O_3 containing HA at 2.5, 5.0, 7.5, and 10 wt% concentrations.

Preparation of Aluminum Oxide–Hydroxyapatite Ceramic Composite Powder

Pure HA powder at four concentrations (2.5, 5.0, 7.5, and 10 wt%) [<200 nm particle size, Lot No.: MKCQ2685, Sigma-Aldrich] was mixed with concentrated nitric acid to form a clear, turbid-free solution. Al_2O_3 powder [≤10 µm particle size, Lot No.: MKCQ4209, Sigma-Aldrich] was then incorporated into the mixture. The resulting solution was placed in an ultrasonic bath for 3 minutes to prevent particle agglomeration and ensure the uniform distribution of HA in Al_2O_3. The mixture was then gradually added to the ammonia solution while continuously stirring with a magnetic stirrer for 2 hours. The solution's pH was maintained at 10. Finally, the mixture was allowed to settle overnight, after which decantation and rinsing with demineralized water were performed. After dehydrating the precipitate for 1 day in a hot air oven at 80°C for 3 hours, it was fired at 850°C for 4 hour and then ground to powder using a mortar.[17] The powder was then passed through a 10 µm sieve (TIMC test sieves, Testing Instruments Manufacturing Company Pvt., Ltd., Kolkata, India) to obtain a uniform particle size. This powder was labeled as AHA ceramic composite core powder.

Preparation of Specimens

The corresponding ceramic powders of each group were mixed with ceramic modeling liquid (VITA modeling fluid, VITA Zahnfabrik, Germany) to form a slurry. The resultant slurry was poured into a cuboidal stainless-steel mold ($5 \times 5 \times 3$ mm^3) using the vibration-condensation method and was uniaxially pressed. It was then dried in an oven preheated to 480°C for 8 minutes until the compacted specimen reached the green stage. The final sintering of the specimen was done at 1200°C for 1 hour (MIHM-VOGT HT-S, Germany). Three sintered specimens ($n = 3$) were fabricated for each group.

Field Emission Scanning Electron Microscopy–Energy Dispersive X-ray Spectroscopy and X-ray Diffraction Analysis

The microstructure and surface topographies of the sintered block specimens of each group were obtained using field emission scanning electron microscopy (FESEM) coupled with energy dispersive X-ray (EDX) spectroscopy (Carl Zeiss, SUPRA 55 VP). One random sintered specimen ($n = 1$) from each group was selected for scanning and imaging. Images were obtained at 25000× magnification. For X-ray diffraction (XRD) analysis (PW3040/60 X'pert Pro PANalytical diffractometer), all three sintered block specimens of each group were ground to powder and scanned continuously for 1 hour using Cu–Kα X-ray radiation at 1.54 Å, 40 kV, 30 mA, with a diffraction angle ranging from 10° ≤ 2θ ≤ 90°, 0.02° step size, and 20 seconds per step. The crystalline structures were determined in comparison to the known standards provided by the Joint Committee on Powder Diffraction Standards (JCPDS) and the International Centre for Diffraction Data (ICDD). The peak intensities were assessed using the Origin data analysis software (OriginLab Corporation, Massachusetts, USA).

Results

The FESEM image of the group A specimen (Fig. 1) showed well-crystallized (≤10 µm) structures that appeared porous with agglomerates. The free-grain surface and boundary were irregular.

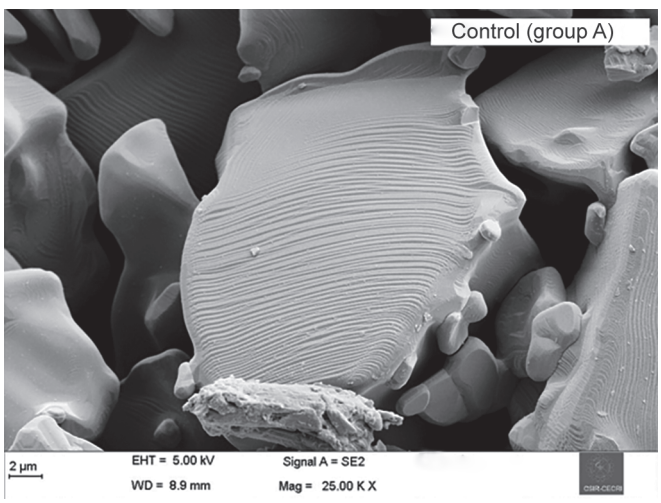

Fig. 1: FESEM image of the control group (group A); 25000× magnification

Groups B to E (Fig. 2) revealed the presence of hexagonal rod-shaped HA crystallites scattered in the Al_2O_3 matrix. With the incorporation of HA, the free-grain surface and boundaries of Al_2O_3 were regular and smooth. Nevertheless, HA incorporation did not affect the pore shrinkage. An increase in the appearance of hexagonal crystallites of nano-HA was observed as the wt% of HA nano-powder increased from the experimental groups B to E. Quantitative (Table 1) and qualitative data (Fig. 3) from the

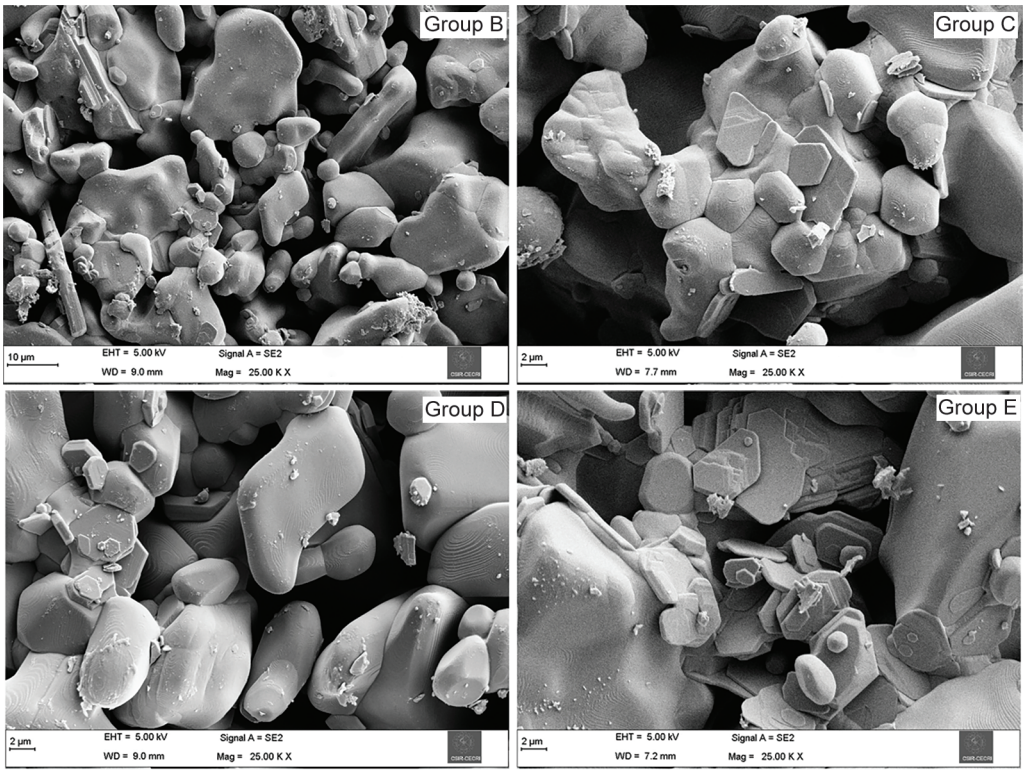

Fig. 2: FESEM images of the experimental groups—groups B, C, D, and E at 25000× magnification

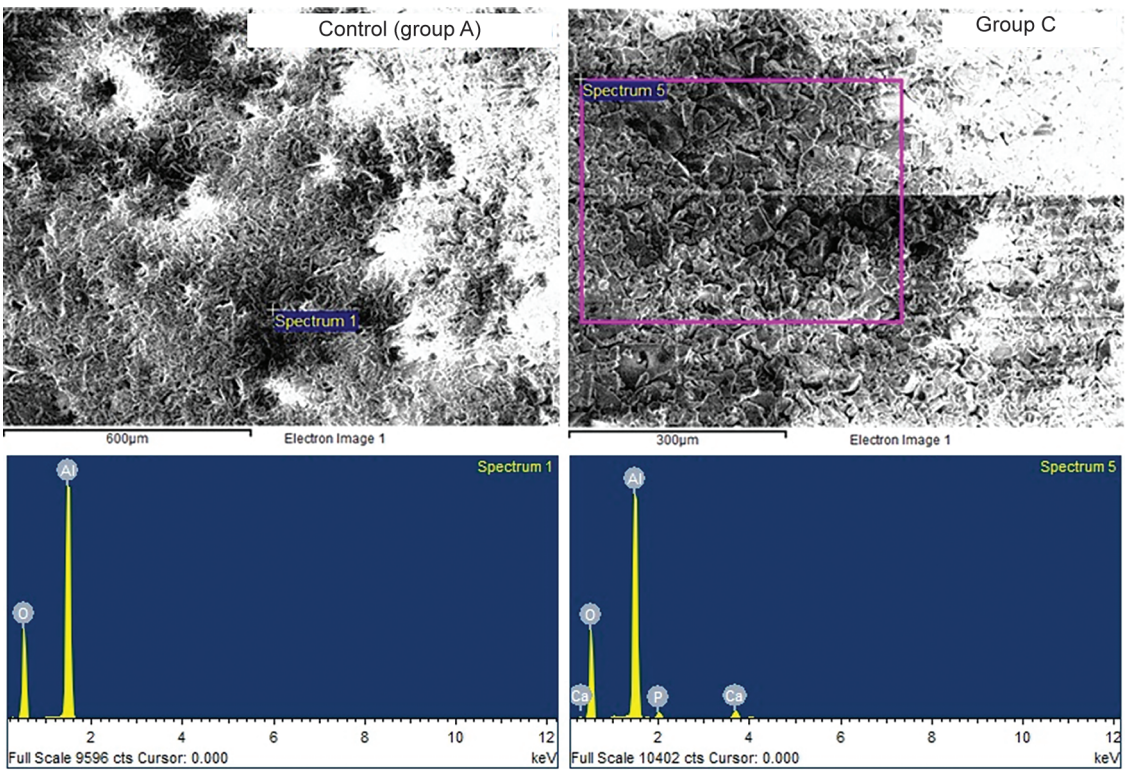

Fig. 3: EDX spectra of the control (group A) and an experimental group (group C)

EDX spectrum of group A showed visible peaks of oxygen (O) and aluminum (Al), whereas the spectra of groups B to E showed visible peaks of calcium (Ca) and phosphorus (P) additionally. This ascertains the presence of HA in the AHA ceramic composites.

The peak intensities of α-Al_2O_3 (JCPDS card 42-1468 and ICDD card 00-010-0173) in crystallographic planes or Miller indices were observed in the XRD spectrum of group A (Fig. 4).

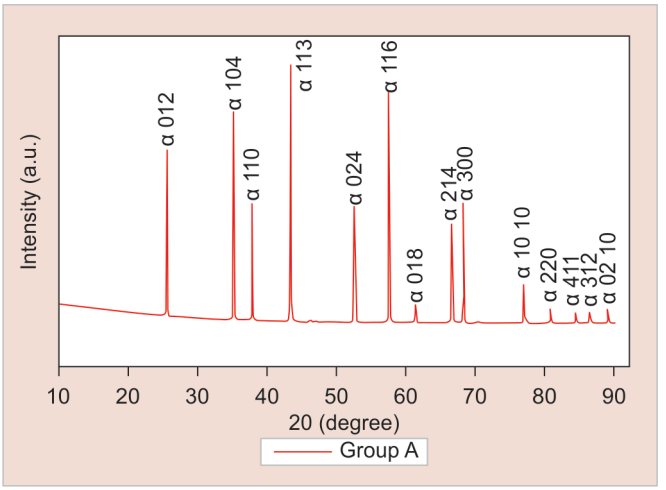

Fig. 4: XRD spectrum of the control group (group A)

There were significant spectral differences between the control and experimental groups. Peaks attributable to Al_2O_3, HA (JCPDS card number 09-0432 and ICDD card 01-073-0293), and a range of calcium aluminate (CA) molecules such as calcium dialuminate/grossite ($CaAl_4O_7$), dodecacalcium hepta-aluminate/mayenite ($Ca_{12}Al_{14}O_{33}$), pseudo-mayenite ($Ca_5Al_6O_{14}$), tricalcium aluminate ($Ca_3Al_2O_6$), and calcium hexa-aluminate [$CaO(Al_2O_3)_6$], were observed in the XRD spectra of groups B to E (Fig. 5). Furthermore, an exclusive phase peak attributed to monocalcium aluminate/krotite ($CaAl_2O_4$) was evident in groups D and E, which was absent in groups B and C. This signified the addition of HA in the Al_2O_3 and the solid-state interaction between Al_2O_3 and HA, yielding various CAs. Moreover, there was viable HA in the ceramics without decomposition. Hence, sintering the Al_2O_3 ceramic matrix with a maximum of 10 wt% HA did not cause its decomposition without degradation by-products.

Table 1: Elemental composition of the groups

	Wt% of elements			
Groups	*O*	*Al*	*P*	*Ca*
A	53.38	46.62	–	–
B	54.68	43.18	0.63	1.51
C	53.99	41.79	1.64	2.58
D	54.56	38.66	2.14	4.64
E	54.36	37.96	2.56	5.13

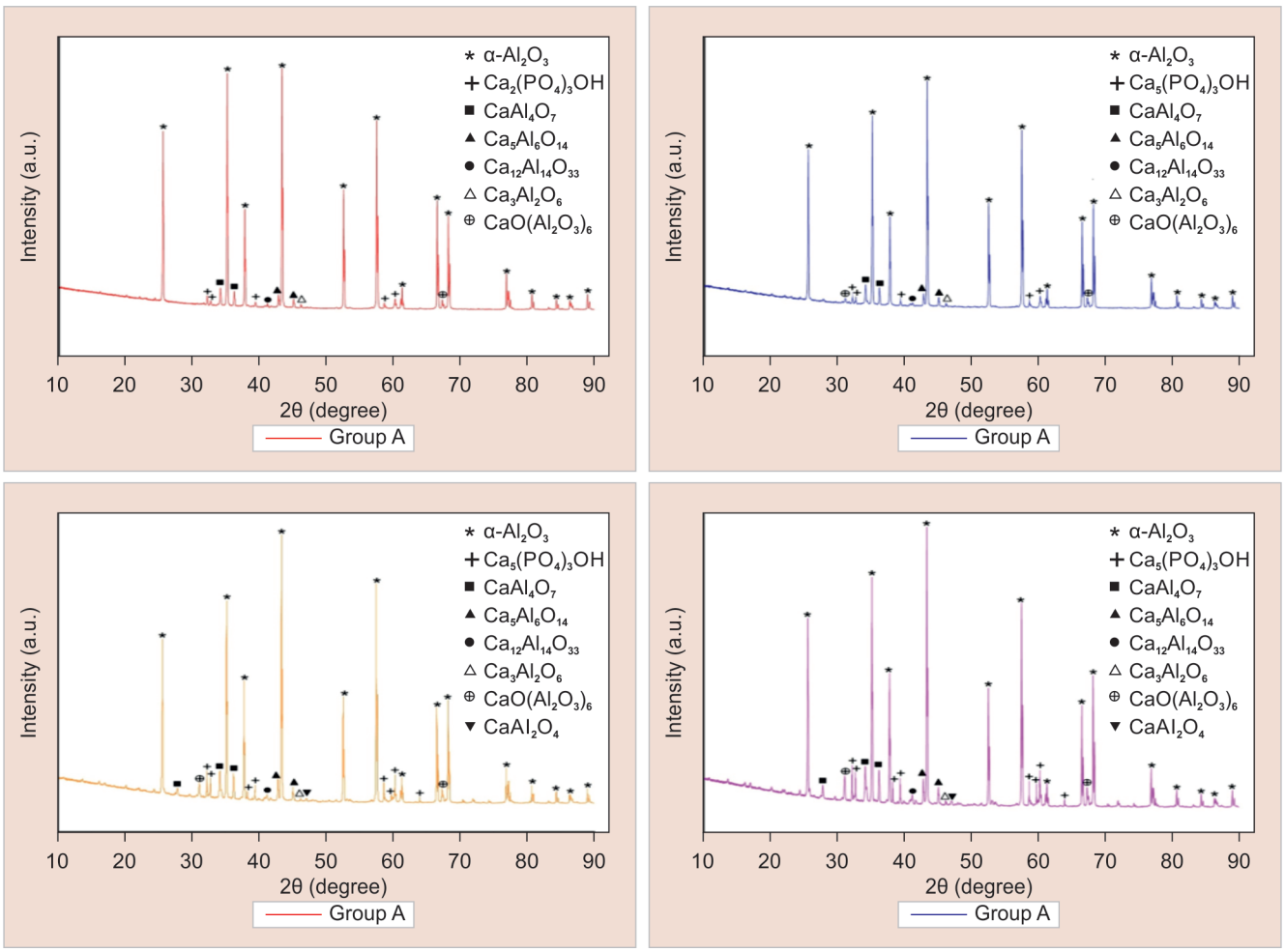

Fig. 5: XRD spectra of the experimental groups—groups B, C, D, and E

Discussion

In the present research, HA nanoparticles were utilized as the medium for bonding the Al_2O_3 ceramic core with the tooth by 10-MDP primers. Hence, the availability of HA nanoparticles after sintering without decomposition is crucial. The topographical evaluation of the AHA ceramic composite specimen by FESEM showed the presence of hexagonal agglomerates of HA, and different molecules of CA were seen surrounded by Al_2O_3 particles. The hexagonal structure consisted of a network of phosphate (PO_4) tetrahedra interconnected by Ca ions interspersed among them, which is similar to the study conducted by Ma and Liu.[18] EDX stoichiometric analysis of AHA ceramic composite specimens revealed the elemental composition of groups A to E. The predominant elements were Al and O, followed by Ca and P, which were also detected in groups B to E since they were included in the precursor. The diffraction peaks from the XRD spectra were found to be a good match to the standards provided by the JCPDS and ICDD for Al_2O_3 and HA. Besides the HA peaks in the XRD spectra of groups B to E, the appearance of various molecules of CA was found as a secondary phase due to the solid-state reaction between Al_2O_3 and HA.

The formation and kinetics of these CAs have been well documented in previous literature.[19] Solid-state reactions for the formation of CA take place by the diffusion of Al from the Al_2O_3 into the HA or Ca from the HA into the Al_2O_3. Ca is known to be the diffusing species in the CaO–Al_2O_3 system.[20] Since the majority of CA intermediate compounds are Al_2O_3-rich, it follows that the reaction proceeds by Ca diffusion from the HA to the Al_2O_3 at the interface, resulting in Al-rich CAs. Ji and Marquis characterized HA reinforced with Al_2O_3 at 1200–1400°C sintering temperatures. The XRD analysis revealed the presence of α-TCP at 1300°C. At elevated temperatures (>1300°C), further decomposition of HA was noted with no evidence of Al_2O_3 being traced. This indicated that Al_2O_3 was completely consumed by solid-state reaction with the formation of various CA molecules evident in the XRD spectra.[21] Viswanath and Ravishankar found no peaks of Al_2O_3 in the XRD spectra when HA was reinforced with Al_2O_3 at 1000°C sintering temperature. This absence of peaks was attributed to the appearance of CA at temperatures starting from 1000°C, and additional peaks were observed as the wt% of Al_2O_3 in the ceramic composite increased. In the composites containing 20 and 30 wt% Al_2O_3, HA started to decompose into TCP [$3Ca_3(PO_4)2$] even at 1000°C as a result of its reactivity with Al_2O_3.[22] The abovementioned studies focused on HA being the major ingredient with Al_2O_3 as a reinforcer.

On the contrary, in the present research, Al_2O_3 served as the major ingredient with HA as the incorporated compound. In contrast to the abovementioned studies, peaks of Al_2O_3 and HA were traced in the XRD spectra of the experimental groups in addition to CA peaks. The nondisappearance of the peaks of Al_2O_3 indicated that it was partially consumed by solid-state reaction with the formation of different formulations of CA. Likewise, the nondecomposition of HA when sintered with Al_2O_3 at 1200°C was attributed to the difference in Al_2O_3–HA ratio with a maximum of 10 wt% of HA incorporated in Al_2O_3.

Muralithran and Ramesh characterized the effect of sintering temperature (1000–1450°C) on the commercially available HA and stated that the XRD traces of specimens sintered below 1350°C showed no evidence of any phase except for HA. However, the presence of α-TCP and β-TCP was revealed at sintering temperatures of 1400 and 1450°C, respectively. This was due to the calcium–phosphate (Ca–P) proportion being identical to the stoichiometric value. If there had been any variation from the stoichiometric value, β-TCP would have formed in the specimens that were sintered at temperatures <1350°C.[23] The result of this present research was found to be congruent with the result of the earlier studies conducted, with the absence of post-sinter degradation products at 1200°C and the Ca–P proportion identical to the stoichiometric value. Sintering of HA at temperatures >1200°C tends to eliminate the hydroxyl ion (OH^-) (dehydroxylation) by losing the water molecule (H_2O) in the HA matrix to form oxyapatite [$Ca_{10}(PO_4)_6(OH)_2$] with a noncharged vacancy.[24,25] There will not be a reverse phase transformation, and this oxyapatite phase is stable.[26] Nevertheless, additional heating to 1450°C may cause HA to break down into α-TCP, β-TCP, TTCP [Ca4P2O9], and CaO.[27]

Numerous studies reported the reaction of HA with ZrO_2. Irrespective of the wt% of ZrO_2 and HA being added, HA started to decompose at 1250°C.[16] Microstructural analysis revealed that there was no significant reaction between ZrO_2 and HA at 1250°C, and the reaction was only significant at temperatures above 1250°C.[16] Lim et al. noted the release of water vapor during the decomposition, which was said to contribute to the hike in the porosity and reduction in the density of the composite.[14] On the contrary, in this present research, the reaction between Al_2O_3 and HA was evident at 1200°C with no water vapor release during the reaction and accompanied by the formation of intermediate compounds of CAs.

The primary focus of this research was to characterize the AHA ceramic composite and to ascertain the availability of HA without decomposition when sintered with Al_2O_3 to aid in chemical bonding with 10-MDP-based resin cements. Fukegawa et al. outlined two chemical binding models of HA with 10-MDP. In the ionic binding model, 10-MDP interacts with the Ca^{2+} ions of HA by either having one of its P-OH groups release an H^+ ion to create a $P–O^-$ group, or by both P–OH groups releasing H^+ ions to generate two $P–O^-$ groups during the electrostatic interactivity with HA. In the covalent binding model, 10-MDP reacts with the PO_4^{3-} ions of HA to produce pyrophosphates.[12] Therefore, with the availability of HA in the AHA ceramics, there would be a chemical or covalent bonding at the adhesive-Al_2O_3 ceramic prostheses interface.

The limitation of the current research is that it neither focuses on the densification of the composite nor the mechanical properties of the AHA ceramic composites when sintered at 1200°C. Moreover, the influence of CA formation on the mechanical properties of the novel AHA ceramic composite needs to be investigated in future research.

Conclusion

Within the limitations, it can be concluded that a quantitative and qualitative increase in the appearance of HA was observed as the concentration of the HA increased from the experimental groups B to E. HA did not decompose at 1200°C when sintered with Al_2O_3, with no traces of post-sinter degradation by-products detected in all the experimental groups. In addition, various molecules of CA were found to appear due to the diffusion of Ca from the HA into the Al_2O_3 matrix.

Author Contributions

BK: supervision, validation, visualization; YFJ: investigation, methodology, writing—review and editing; AR: conceptualization, data curation, formal analysis, writing—original draft.

Data Availability Statements

Data is available on request.

Orcid

Kandasamy Balu https://orcid.org/0009-0004-7886-0155
Jailaudeen Yasmin-Fathima https://orcid.org/0009-0001-5079-5177
Ranganathan Ajay https://orcid.org/0000-0001-9315-8912

References

1. Gonzaga CC, Okada CY, Cesar PF, et al. Effect of processing induced particle alignment on the fracture toughness and fracture behavior of multiphase dental ceramics. Dent Mater 2009;25(11):1293–1301. DOI: 10.1016/j.dental.2009.03.013
2. Rizkalla AS, Jones DW. Mechanical properties of commercial high strength ceramic core materials. Dent Mater 2004;20(2):207–212. DOI: 10.1016/s0109-5641(03)00093-9
3. Blatz MB, Sadan A, Kern M. Resin-ceramic bonding: a review of the literature. J Prosthet Dent 2003;89(3):268–274. DOI: 10.1067/mpr.2003.50
4. Nagaoka N, Yoshihara K, Feitosa VP, et al. Chemical interaction mechanism of 10-MDP with zirconia. Sci Rep 2017;7:45563. DOI: 10.1038/srep45563
5. Atsu SS, Kilicarslan MA, Kucukesmen HC, et al. Effect of zirconium-oxide ceramic surface treatments on the bond strength to adhesive resin. J Prosthet Dent 2006;95(6):430–436. DOI: 10.1016/j.prosdent.2006.03.016
6. Amaral R, Ozcan M, Bottino MA, et al. Microtensile bond strength of a resin cement to glass infiltrated zirconia-reinforced ceramic: the effect of surface conditioning. Dent Mater 2006;22(3):283–290. DOI: 10.1016/j.dental.2005.04.021
7. Zhang Y, Lawn BR, Rekow ED, et al. Effect of sandblasting on the long-term performance of dental ceramics. J Biomed Mater Res B Appl Biomater 2004;71(2):381–386. DOI: 10.1002/jbm.b.30097
8. Azari A, Nikzad Jamnani S, Yazdani A, et al. Deposition of crystalline hydroxyapatite nanoparticles on Y-TZP ceramic: a potential solution to enhance bonding characteristics of Y-TZP ceramics. J Dent (Tehran) 2017;14(2):62–68. PMID: 29104596.
9. Pepla E, Besharat LK, Palaia G, et al. Nano-hydroxyapatite and its applications in preventive, restorative and regenerative dentistry: a review of literature. Ann Stomatol (Roma) 2014;5(3):108–114. DOI: 10.11138/ads/2014.5.3.108
10. Mohsen CA, Abu-Eittah MR, Hashem RMM. The antibacterial and antifungal effect of silver nanoparticles and silver hydroxyapatite nanoparticles on dental ceramic. Rep opinion 2015;7(7):83–88.
11. Katamish HA, Karaksy AO, el-Mahallawy OS. The effect of the dissolution process of hydroxyapatite added to conventional dental porcelain on its mechanical strength. Egypt Dent J 1995;41(2):1085–1094. PMID: 9497644.
12. Fukegawa D, Hayakawa S, Yoshida Y, et al. Chemical interaction of phosphoric acid ester with hydroxyapatite. J Dent Res 2006;85(10):941–944. DOI: 10.1177/154405910608501014
13. Ong JL, Chan DC. Hydroxyapatite and their use as coatings in dental implants: a review. Crit Rev Biomed Eng 2000;28(5–6):667–707. DOI: 10.1615/critrevbiomedeng.v28.i56.10
14. Lim KF, Muchtar A, Mustaffa R, et al. Synthesis and characterization of hydroxyapatite-zirconia composites for dental applications. Asian J Sci Res 2014;7(4):609–615. DOI: 10.3923/ajsr.2014.609.615
15. Towler MR, Gibson IR. The effect of low levels of zirconia addition on the mechanical properties of hydroxyapatite. J Mater Sci Lett 2001;20(18):1719–1722. DOI: 10.1023/A:1012435124012
16. Kutty MG, Bhaduri S, Bhaduri SB. The effects of zirconia additions on the sintering behaviour and phase tability of hydroxyapatite ceramics. Ceram Eng Sci Proc 2001;22(4):601–606. DOI: 10.1002/9780470294703.ch68
17. Singh A, Purohit KM. Chemical synthesis, characterization and bioactivity evaluation of hydroxyapatite prepared from garden snail (Helix aspersa). J Bioprocess Biotechniq 2011;1:1–5. DOI: 10.4172/2155-9821.1000104
18. Ma G, Liu XY. Hydroxyapatite: hexagonal or monoclinic? Cryst Growth Des 2009;9(7):2991–2994. DOI: 10.1021/cg900156w
19. Singh VK, Ali MM, Mandal UK. Formation kinetics of calcium aluminates. J Am Ceram Soc 1990;73(4):872–876. DOI: 10.1111/j.1151-2916.1990.tb05128.x
20. Kohatsu I, Brindley GW. Solid state reaction between CaO and α-Al_2O_3. Z Phys Chem 1968;60:79–89. DOI: 10.1524/zpch.1968.60.1-6.079
21. Ji H, Marquis PM. Preparation and characterization of Al_2O_3 reinforced hydroxyapatite. Biomaterials 1992;13(11):744–748. DOI: 10.1016/0142-9612(92)90011-c
22. Viswanath B, Ravishankar N. Interfacial reactions in hydroxyapatite/alumina nanocomposites. Scr Mater 2006;55(10):863–866. DOI: 10.1016/j.scriptamat.2006.07.049
23. Muralithran G, Ramesh S. The effect of sintering temperature on the properties of hydroxyapatite. Ceram Int 2000;26(2):221–230. DOI: 10.1016/S0272-8842(99)00046-2
24. Juang HY, Hon MH. Fabrication and mechanical properties of hydroxyapatite-alumina composites. Mater Sci Eng C 1994;2(2):77–81. DOI: 10.1016/0928-4931(94)90033-7
25. Kijima T, Tsutsumi M. Preparation and thermal properties of dense polycrystalline oxyhydroxyapatite. J Am Ceram Soc 1979;62(9–10):455–460. DOI: 10.1111/j.1151 - 2916.1979.tb19104.x
26. Zhou J, Zhang X, Chen J, et al. High temperature characteristics of synthetic hydroxyapatite. J Mater Sci: Mater Med 1993;4:83–85. DOI: 10.1007/BF00122983
27. Wu JM, Yeh TS. Sintering of hydroxylapatite-zirconia composite materials. J Mater Sci 1998;23:3771–3777. DOI: 10.1007/BF00540526